

# TechFacts

**#104**

Internal arcs in clean air

2023/08, rev. 1.0



Blue technology  
with Zero F-gases

# 1 Introduction

On the way to a CO<sub>2</sub>-neutral energy supply, there has been an increased demand for sustainable technologies for the generation, transmission, and distribution of electrical energy. For transmission networks, this means the use of sulfur hexafluoride (SF<sub>6</sub>)-free equipment, with the most common alternative insulating media being natural gases. Amongst these gases, the climate-neutral and greenhouse-gas-free technical air (clean air), composed of 80 % Nitrogen (N<sub>2</sub>) and 20 % Oxygen (O<sub>2</sub>), provides many advantages, such as easy and riskless gas handling, chemical stability, and low chemical interaction with other materials. Clean air as insulation gas, in combination with the vacuum interrupter technology for interruption of load and fault currents, is an excellent choice to replace the SF<sub>6</sub> gas as an insulating and interruption medium. It is already commonly used in high-voltage switchgear applications today. The use of this technology requires an investigation of the behavior of clean air in the unlikely event of an internal arc fault in transmission equipment such as air-insulated (AIS) and gas-insulated switchgear (GIS).

An internal arc fault leads to mechanical and thermal stresses on the enclosure of the switchgear. Thereby, the arc fault process, which causes an overpressure and local overheating, is mainly influenced by the used insulating gas. Compared to SF<sub>6</sub> gas, the pressure build-up and the gas flow are different in clean air. Simulation and test results show that in the unlikely event of an internal arc fault in the switchgear enclosure, the gradient of the pressure rise is significantly higher if clean air is used instead of SF<sub>6</sub> gas. The pressure increase can be controlled by using a commercially available suitable pressure relief device, e.g., a rupture disc. When compared to SF<sub>6</sub>, such a rupture disc will open earlier in clean air, owing to a faster pressure rise. A rapid pressure drop in the switchgear housing will follow, due to the very steep pressure

drop gradient of clean air, which ultimately leads to a lower maximum pressure value and lower stress to the whole equipment.

# 2 Requirements and standards

The occurrence of an internal arc fault in a GIS compartment is an exceptional case in which, after a dielectric breakdown, the electrical energy of the short-circuit current is mainly converted into thermal and radiation energy. This energy is responsible for the vaporization of metallic and insulating materials, as well as the expansion of the mixture of vapor and insulating fluid in the compartment.

Rated short-circuit current	Protection stage	Duration of current	Performance criteria
< 40 kA	1	0.2 s	No external effect other than the operation of suitable pressure relief devices
	2	≤ 0.5 s	No fragmentation (burn-through is acceptable)
≥ 40 kA	1	0.1 s	No external effect other than the operation of suitable pressure relief devices
	2	≤ 0.3 s	No fragmentation (burn-through is acceptable)

Table 1: Overview of performance criteria.

The internal arc may also burn through the enclosure. Fortunately, the internal arc fault is a very sporadic event. But even for these cases, a GIS and all its compartments must be designed to afford a certain protection level to operating personnel and equipment in its vicinity. The GIS enclosure must therefore limit the external effects of an internal arc fault. The international standards IEEE Std. C37.122 [1] and IEC 62271-203 [2] define common performance criteria for internal arc fault tests (Table 1).

The duration of the arc current, as given in Table 1, is related to the protection system. There are two protection stages defined: the first stage or main stage, and the second stage or back-up protection. Moreover, there are general requirements not addressed by the above shown table: the arc must not disperse into adjacent compartments; in case of burn-through, a hole or tear may appear (Figure 1), whereas fragmentation is strictly forbidden (Figure 2).



Figure 2: Hole and tear in a GIS enclosure.



Figure 2: Fragmentation at a GIS enclosure.

A pressure relief device, the before-mentioned rupture disc, is commonly installed to protect the compartment from fragmentation. This rupture disc must be designed to withstand the overpressure inside, under any allowable ambient and load conditions, but must also safely release the quick rising overpressure in case of an internal arc fault. The outlet must be designed to release as quickly as necessary to avoid critical overstressing of the enclosure structure. The internal arc fault test on GIS compartments is a valued test to verify a standardized safety margin for GIS compartments.

## 3 Test and measurement

### 3.1 Test setup and test object

Figure 3 shows a typical test set-up of an internal arc test in clean air [3]. The test object was a single pole of a three-pole-operated outdoor dead tank vacuum circuit-breaker.

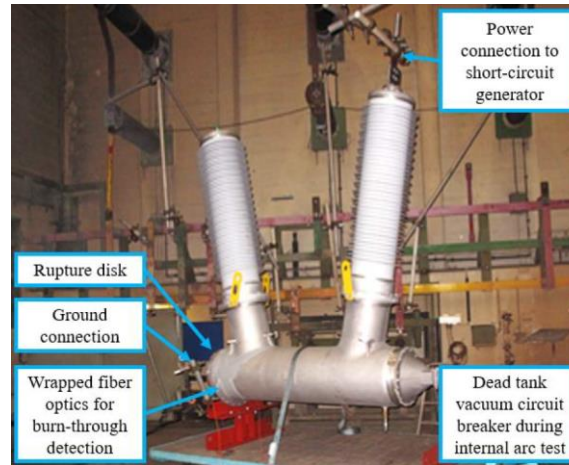


Figure 3: Photo of the test set-up during internal arc test at a dead tank circuit-breaker pole.

The pole was equipped with a rupture disc as a pressure relief device. Fiber optic cables were used for the monitoring of burn-through events of the enclosure and of the response of the rupture disc. One fiber optic cable was secured across the rupture disc to detect the response by loss of light signal (see Figure 4).

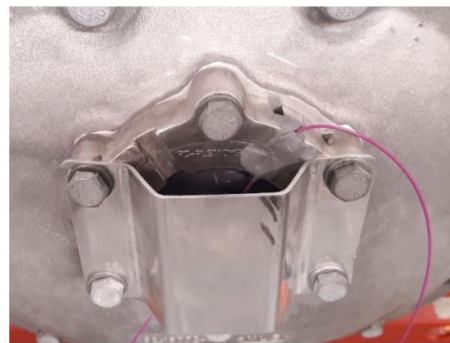


Figure 4: Rupture disc with guard plate before operation with fiber optic cable to detect operation.

A second fiber optic cable was wrapped around the enclosure, in the area of a potential burn-through (see Figure 3). The short-circuit current was supplied through one of the bushings. The internal fault was initiated by an ignition wire (see Figure 5) at the end of the enclosure, in order to minimize the movement of the arc.

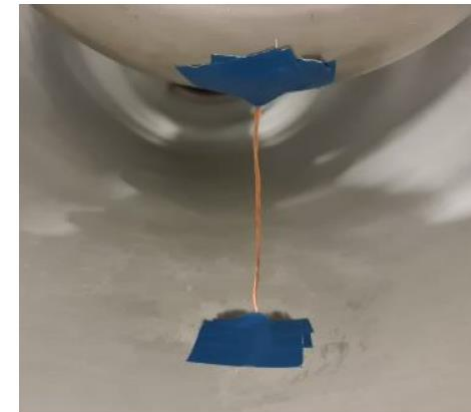


Figure 5: Ignition wire to initiate an internal arc fault.

The dead tank vacuum circuit-breaker was connected to the short-circuit generator via the contact tube in the right bushing. The vessel was grounded on the left side.

### 3.2 Test execution and test results

The short-circuit current for the test was supplied by a short-circuit generator directly to the test object. As mentioned in section 3.1, the current was fed through one bushing, went through the ignition wire/arc to the enclosure and back to the source. The test object was isolated from ground to avoid current flow through the grounding system of the test laboratory and to ensure that the test current was accurately measured in the return conductor by a Rogowski coil. The voltage across the test object (arc voltage) and the pressure inside the

test object were also measured. As indicated in section 3.1, the output from two fiber optic cables was monitored during the test to detect rupture disc operation and burn-through of enclosure.

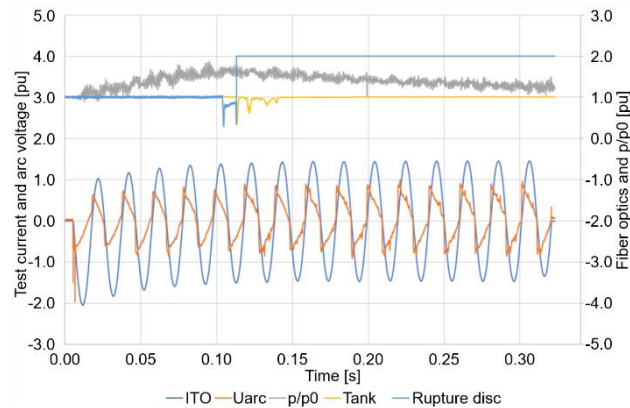


Figure 6: Ignition wire to initiate an internal arc fault.

Figure 6 shows an oscillogram of the internal arc test ( $U_{arc}$  is the voltage across the test object,  $I_{TO}$  is the current through the test object,  $p/p_0$  is the pressure in the test object).

The test current of 40 kA at a driving source voltage of 10 kV was provided for 316 ms. The peak factor of short-circuit-current at short-circuit initiation was determined to be 2.0 p.u. (required  $\geq 1.7$  p.u.). There was a measured maximum pressure inside the enclosure of 1.6  $p/p_0$ . The operation of the rupture disc was detected 108 ms after short-circuit initiation. The enclosure did not burn through. The test was successful and the pressure inside remained far below the critical structural limits of the affected compartment. The requirements of the international standards IEEE Std. C37.122 [1] and IEC 62271-

203 [2] have been fulfilled in terms of test parameters and test results.

## 4 Modelling and simulation

### 4.1 Basics of modelling

As mentioned previously, the pressure build-up during the arc fault process can be controlled by overpressure protection systems. Their technical design can be supported by arc fault simulations, for which there are many approaches available in the literature. According to [4] these simulation approaches can be classified into three groups, according to their application area:

- (I) Closed compartments,
- (II) Compartments with openings to the environment and
- (III) Compartments with attached rooms enabling a pressure release via openings.

The simulation approach for the first group describes the involved compartments by their effective volume and the pressure increase is computed as a function of the electrical energy, see e.g. [5].

In the case of the second group, the simulation approach from group (I) is extended by the consideration of the exhaust of gas through the opening into the environment, see e.g. [4]

In [6], a simulation approach based on the conservation of mass and energy in a control volume is described in detail. This approach allows the connection, via openings, of an arbitrary number of compartments or rooms to each other and to the environment and can be used for groups (II) and (III) as well.

Further developments to the mentioned simulation approaches are the following:

- A multi-domain approach using Simcenter Amesim<sup>1</sup>
- A computational fluid dynamics (CFD) approach using ANSYS® Fluent.

In the next two chapters the simulation of internal arcs in clean air with these approaches is presented.

### 4.2 Arc fault simulation with Amesim

Amesim is a recent simulation software for the modeling and analysis of multi-domain systems. Using the physical library fluids, an arbitrary number of volumes can be considered, and the mass and enthalpy flow via openings between them can be simulated.

Figure 7 shows the equivalent circuit diagram for the test set-up of Figure 3 [3]. The tested vacuum dead tank circuit-breaker is represented by volume  $V_1$  and the environment by volume  $V_3$ . The arc power  $P_{arc}$  is injected in  $V_1$  as a function of time. During the simulation, the pressure build-up in  $V_1$  is evaluated, and the rupture disc is released if  $p_1$  exceeds the opening pressure  $p_{open}$  of the rupture disc.

The arc fault process in the tested vacuum dead tank circuit-breaker has been simulated for the current trend shown in Figure 6, with parameters taken from [5].

<sup>1</sup> Simcenter Amesim is a commercial simulation software for the modeling and analysis of multi-domain systems. It is part of systems engineering domain and falls into the mechatronic engineering field.

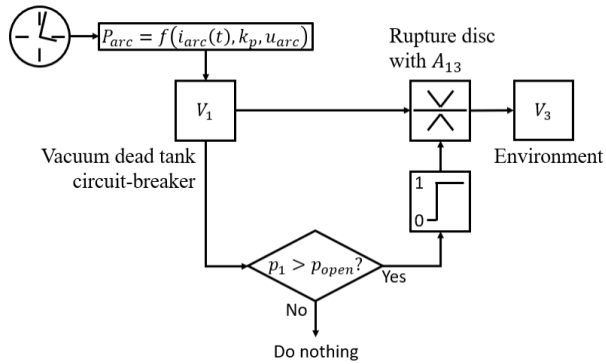


Figure 7: Equivalent circuit diagram for the test set-up in Figure 3.

Figure 8 shows the comparison of the simulated and measured pressure in volume  $V_1$ .

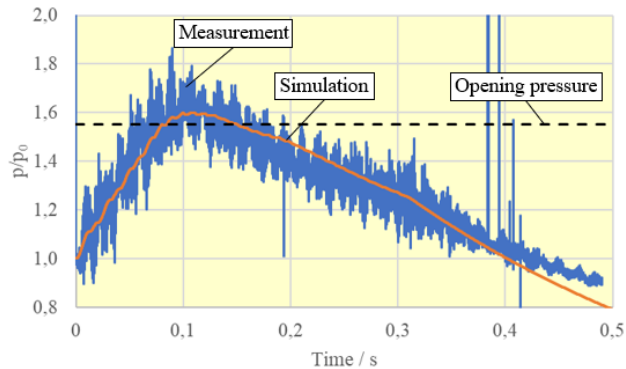


Figure 8: Comparison of simulated and measured pressure in volume  $V_1$ .

As can be seen, the pressure increases very fast while the rupture disc is closed. After the response of the pressure relief valve, the pressure drops before the test current is switched-off at about 0.35 s (see Figure 6). This

indicates that the pressure protection system is well-designed and works as expected. The comparison in Figure 8 shows a good agreement between measurement and simulation, thus validating the multi-domain approach using Simcenter Amesim.

### 4.3 Arc fault simulation with Fluent

A CFD arc fault simulation tool based on ANSYS® Fluent software was developed. It doesn't require an input for the thermal transfer coefficient and the arc voltage, as the arc fault process is simulated using a three-dimensional arc model, including a sub model describing the radiative transfer inside the arc and from the arc to the surrounding gas. The implementation of the arc fault model in different insulating media is illustrated in Figure 9.

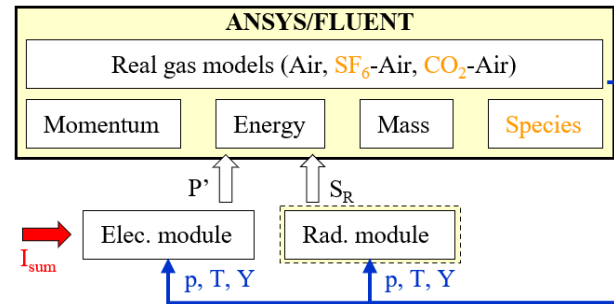


Figure 9: Link of conservation equations and sub models via source terms and scalar quantities.

The radiative transfer from the arc into its environment is reflected by an appropriate source term in the energy equation. This source term is calculated in the radiation module using the Discrete Ordinate Model. Another source term in the energy equation governs the Joule effect and is obtained through the electric module. This source term is evaluated with a varying arc radius.

To simulate the plasma flow, thermodynamic and transport properties of the insulating media must be provided to the ANSYS® Fluent solver. This is realized by available real gas models for pure *Air* and the mixtures  $SF_6 - Air$  and  $CO_2 - Air$ , based on the assumption of local thermodynamic equilibrium (LTE). The scalar quantities pressure  $p$ , temperature  $T$  and mass fraction  $Y$  ( $SF_6$  or  $CO_2$ ) in the cases of  $SF_6 - Air$  or  $CO_2 - Air$  mixtures are the input variables to the radiation module and the electric module, see Figure 9. A macro has been developed to take into account the operation of the rupture disc, see Figure 10.

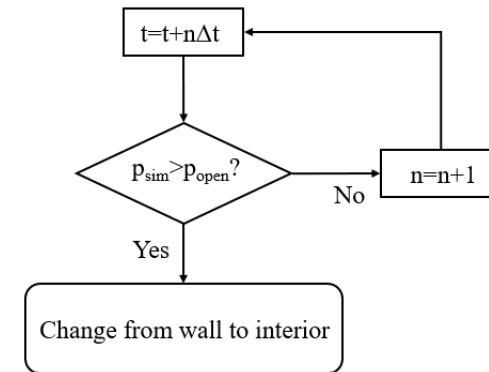


Figure 10: Flow chart of macro for rupture disc operation.

The rupture disc opens at a pre-defined response pressure  $p_{open}$ . At the end of each simulation time step, the average surface pressure value  $p_{sim}$  is estimated at the rupture disc wall and compared with  $p_{open}$ . If  $p_{sim}$  exceeds  $p_{open}$  the rupture disc wall is changed from "wall" to "interior" and the vessel volume is connected to the surroundings. The CFD arc fault simulation tool based on the ANSYS® Fluent software has been validated by using a type test of a GIS filled with clean air [7]. Figure 11 illustrates the discretized vessel without the surrounding solution domain.

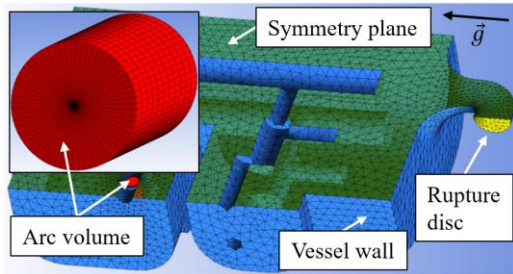


Figure 11: Half model of the regarded vessel with discretized arc volume.

Using  $I_{sum}(t)$  depicted in Figure 12, the arc fault process has been simulated for an arcing time of 0.5 s, including the opening of the rupture disc and the following outflow of hot Air to the surroundings.

For validation purposes concerning the type test, Figure 13 shows the comparison of measured and simulated arc voltage. The simulated arc voltage is nearly constant following the input by the sum current, in contrast to the oscillating measured arc voltages. The comparison of the pressure build-up within the gas-insulated switchgear is illustrated in Figure 14.

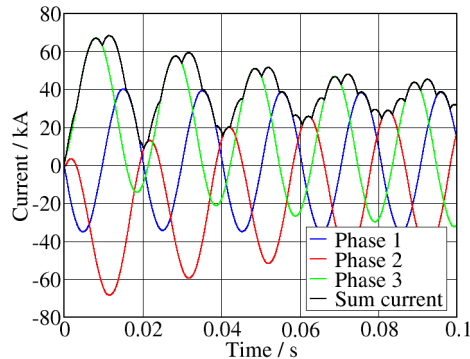


Figure 12: Three-phase currents and sum current from the type test.

Figures 13 and 14 demonstrate a good agreement between measurement and simulation, thus validating the CFD arc fault simulation tool based on ANSYS® Fluent.

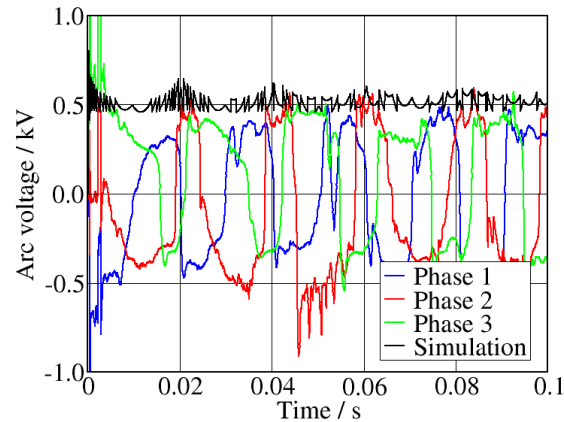


Figure 13: Comparison of measured and simulated arc voltage.

Additionally, the arc fault process was simulated with  $CO_2$  and  $SF_6$ , under the same conditions, in order to investigate the influence of the insulating media. The operation of the rupture disc and the subsequent outflow of hot gas to the surroundings influences the arc fault process significantly and changes the behavior of the pressure build-up within the gas-insulated switchgear, see Figure 14. While the rupture disc is closed, the arc fault process is mainly influenced by the heat capacity of the arc of the respective gas. As clean air features the smallest arc heat capacity, see [7], the pressure rises very fast when compared with  $CO_2$  and  $SF_6$ .

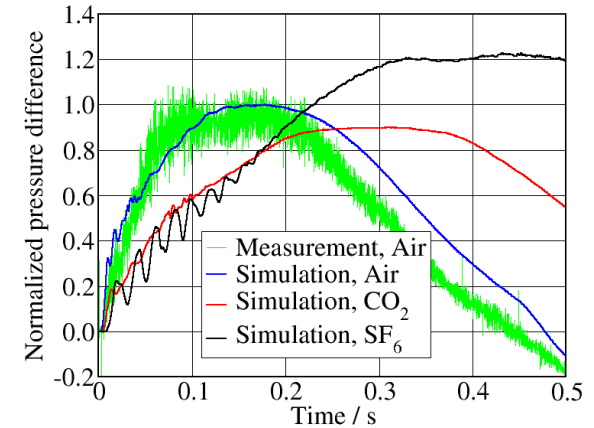


Figure 14: Pressure build-up in the gas-insulated switchgear (normalized to the maximum value in the simulation with clean air).

After the opening of the rupture disc, the outflow of the hot gas is mainly influenced by the speed of sound, which is inversely proportional to the gas density. In the compared simulation variants, the initial pressure is the same and the gas density differs very strongly. The highest gas density is that of  $SF_6$  and the hot gas flows out with the lowest speed of sound, see Figure 15.

The highest value for the speed of sound occurs in clean air, while the value for  $CO_2$  lies in between. The pressure curves in Figure 14 can be explained by the described differences in arc heat capacity and speed of sound. In the case of clean air, the arc fault process results in the steepest pressure rise but, due to the enforced outflow of hot gas, the maximum of pressure is reached very rapidly and is then followed by a strong drop of pressure. In the case of  $SF_6$ , the pressure rises much slower, but the outflow of the hot gas is affected by the low speed of sound, leading to a higher maximum of pressure. The lowest values for the maximum pressure are attained for  $CO_2$ .

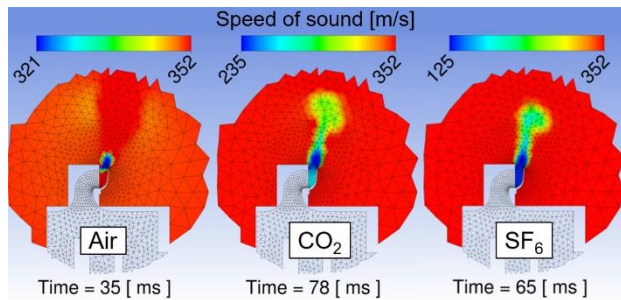


Figure 15: Contour plot of speed of sound in the symmetry plane about 5ms after opening of rupture disc.

## 5 Conclusion and recommendations

The internal arc fault test performed at the single pole of a three-pole-operated dead tank vacuum circuit-breaker showed that in the case of an internal arc in clean air, the latter insulating medium does not behave more critically than  $SF_6$  gas or  $CO_2$ , even though the pressure increase in the enclosure is steeper. The test demonstrated that a properly designed pressure relief device can be applied to effectively limit the pressure rise caused by the internal arc and keep its value well below those of the structural limits of the compartment. The activation of this device reliably protects the gas-insulated compartment from fragmentation and provides confidence in its safe use, which is well-known from  $SF_6$  insulated compartments.

A model of the arc fault process has been developed with the simulation tool Simcenter Amesim. The proposed model has been validated by measured signals for the pressure build-up. It is shown that there is a good agreement between measurement and simulation. The

model can be applied to investigate the pressure build-up in compartments with different volumes and for different short-circuit current values and durations.

A 3D CFD arc fault simulation tool developed on ANSYS® Fluent has also been studied. The arc fault process in a gas-insulated switchgear filled with clean air was simulated. The model was validated by the comparison of measured signals for arc voltage and pressure build-up with the respective simulation results. This tool allows the investigation of the influence of different insulating media on the arc fault process. As such, the arc fault process in the GIS was also simulated with  $CO_2$  and  $SF_6$  under the same conditions. It could be shown that the pressure build-up within the vessel is mainly influenced by the arc heat capacity of the respective gas if the rupture disc is closed. After the opening of the rupture disc, the outflow of the hot gas is mainly influenced by the speed of sound of the gas. If the same initial pressure within the vessel is considered for all regarded insulating media, the highest pressure build-up occurs for  $SF_6$  followed by Air and then  $CO_2$ .

## 6 Bibliography

Author: Dr.-Ing. habil. Frank Reichert

- [1] IEEE Std. C37.122 IEEE Standard for High Voltage Gas-Insulated Substations Rated Above 52 kV.
- [2] IEC 62271-203 Edition 2.0 High-voltage switchgear and controlgear – Part 203: Gas-insulated metal-enclosed switchgear for rated voltages above 52 kV.
- [3] F. Reichert et al.: Investigation on internal arc faults in high-voltage equipment with technical air as insulating medium. 41. CIGRE International Symposium, 1238, 2021.
- [4] M. Anantavanich: Calculation of Pressure Rise in Electrical Installations due to Internal Arcs Considering  $SF_6$ -Air Mixtures and Arc Energy Absorbers, Thesis, RWTH Aachen, 2010.
- [5] G. Friberg. et al.: Calculation of pressure rise due to arcing faults, IEEE Transactions on Power Delivery, Vol. 14, No. 2, pp. 365-370, 1999.
- [6] N. Uzelac et al.: Tools for the simulation of the effects of the internal arc in transmission and distribution switchgear. Cigre, Technical Brochures, 602, WG A3.24, 2014.
- [7] F. Reichert et al.: 3D CFD arc fault simulation in gas-insulated switchgears. Plasma Physics and Technology 6 (1):35–38, 2019.

**Published by**

Siemens Energy Global GmbH & Co. KG  
Grid Technologies  
Siemenspromenade 9  
91058 Erlangen  
Germany

For more information, please visit our website:

[siemens-energy.com](https://www.siemens-energy.com)

or contact us

Email: [support@siemens-energy.com](mailto:support@siemens-energy.com)

Subject to changes and errors. The information given in this document only contains general descriptions and/or performance features which may not always specifically reflect those described, or which may undergo modification in the course of further development of the products. The requested performance features are binding only when they are expressly agreed upon in the concluded contract.

Siemens Energy is a trademark licensed by Siemens AG.

**For the U.S. published by**

Siemens Energy, Inc  
Grid Technologies  
8841 Wadford Drive  
Raleigh, NC 27616  
USA